Chapter 5

Optical Scanning Holography: Advances

5.1 Coherent and Incoherent Holographic Processing

In chapter 4, we have discussed some applications that employ optical scanning holography (OSH). OSH has been implemented by the two-pupil optical heterodyne scanning image processor that we have discussed in chapter 3 [see Fig. 3.11]. All of our discussions regarding the applications that we use OSH have so far been confined to incoherent image processing, i.e., the objects that are processed are incoherent and this leads to some of the important applications of 3-D fluorescence microscopy and remote sensing. Coherent 3-D imaging, nevertheless, is an important extension of the processor in biological imaging for the area of *quantitative phase-contrast imaging* [Cuche, Bevilacqua, and Depeursinge (1999)].

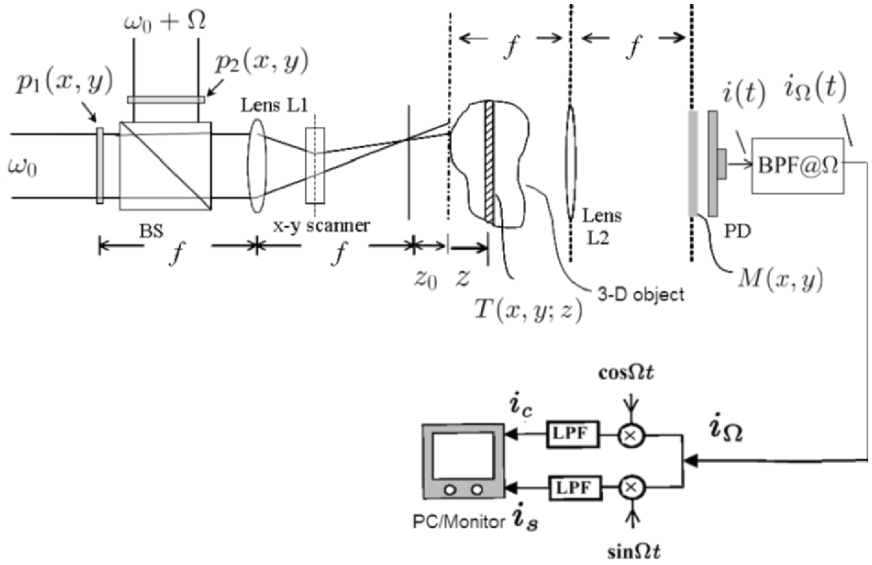

Fig. 5.1 Generalized two-pupil image processor. Adapted from T.-C. Poon, J. Holography Speckle 1, 6-25 (2004).

In this section, we will discuss how the image processor can be configured (or generalized) in order to work in a coherent mode, i.e., the amplitude instead of the intensity of the object can be processed. We shall use Fourier optics discussed in chapter 2, in order to fully analyze the processor.

The generalized processor is shown in Fig. 5.1 with its usual two-pupil set-up for optical scanning of the 3-D object. As compared to the standard setup shown in Fig. 3.11, note that the Fourier transform lens, L2, and the mask, $M(x,y)$, are the additional elements in the system. We will model the 3-D object as a stack of transverse slices where each slice of the object is represented by an amplitude transmittance, $T(x,y;z)$, which is thin and weakly scattering. We will place the 3-D object in front of the Fourier transform lens, L2. $M(x,y)$ is a mask located at the back focal plane of lens L2. The photodetector, PD, collects all the light transmitted by the mask and delivers the processed and scanned current, $i(t)$, as output of the system. Finally, for the usual multiplexing electronic detection the bandpass filter (BPF) is tuned to Ω to give the heterodyne current, $i_\Omega(t)$. By using Fourier optics, we shall outline the procedures used to obtain $i(t)$ upon scanning the object.

The amplitude distribution of the light field, at position z just before the object slice, is given by

$$P_1(x,y;z+z_0)\exp(j\omega_0 t) \; + \; P_2(x,y;z+z_0)\exp[j(\omega_0+\Omega)t]\,, \quad \text{(5.1-1a)}$$

where, according to Fresnel diffraction,

$$P_i(x,y;z+z_0) = \mathcal{F}\{p_i(x,y)\}_{k_x=\frac{k_0 x}{f},k_y=\frac{k_0 y}{f}} * h(x,y;z+z_0) \qquad \text{(5.1-1b)}$$

with $i = 1$ or 2 and $p_i(x,y)$ is the pupil functions shown in Fig. 5.1.

According to the principle of optical scanning developed in section 3.1, the field just after the object slice is

$$\chi(x',y',x,y;z) = \{P_1(x',y';z+z_0)\exp(j\omega_0 t)$$

$$+ \; P_2(x',y';z+z_0)\exp[j(\omega_0+\Omega t]\}T(x'+x,y'+y;z), \qquad \text{(5.1-2)}$$

where $x = x(t)$ and $y = y(t)$ represent the instantaneous 2-D position of the object with respect to the incident light amplitude distribution. This field then propagates through the Fourier transform lens, L2, and reaches the mask, $M(x,y)$. According to Eq. (2.4-5), the field just before the mask, apart from some inessential constant, is

$$\exp[-j\frac{k_0 z}{2f^2}({x_m}^2+{y_m}^2)]$$

$$\times\int\int\chi(x',y',x,y;z)\exp[j\frac{k_0}{f}(x'x_m+y'y_m)]dx'dy',$$

where we have set $d_0 = f - z$ in Eq. (2.4-5) to obtain the phase factor in front of the integral. x_m and y_m are the coordinates in the plane of the mask. The above field is caused by a single object slide. For a 3-D object, we need to integrate the above field over the thickness, z, of the 3-D object to find the total field just before the mask. This becomes the following expression

$$\int\Big\{\exp[-j\frac{k_0 z}{2f^2}({x_m}^2+{y_m}^2)]$$

$$\times\int\int\chi(x',y',x,y;z)\exp[j\frac{k_0}{f}(x'x_m+y'y_m)]dx'dy'\Big\}dz.$$

By multiplying the above field by the mask, the field, just after the mask is then given by

$$\psi(x,y;x_m,y_m)=\Big\{\int\Big[\exp[-j\frac{k_0 z}{2f^2}({x_m}^2+{y_m}^2)]$$

$$\times\int\int\chi(x',y',x,y;z)\exp[j\frac{k_0}{f}(x'x_m+y'y_m)]dx'dy'\Big]dz\Big\}M(x_m,y_m).$$

Finally, the photodetector, PD, which responds to intensity, gives the current output $i(t)$ by spatially integrating the intensity:

$$i(t)\propto\int|\psi(x,y;x_m,y_m)|^2dx_m dy_m\ .$$

$i(t)$ consists of a baseband current and a heterodyne current at a frequency of Ω. After some manipulations, the heterodyne current, $i_\Omega(t)$, at the output of a bandpass filter [see Fig. (5.1)], becomes

$$i_\Omega(t)\propto\int[P_1(x',y';z'+z_0)P_2^*(x'',y'';z''+z_0)\exp(-j\Omega t)$$

$$+P_2(x',y';z'+z_0)P_1^*(x'',y'';z''+z_0)\exp(j\Omega t)]$$

$$\times\exp\{j\frac{k_0}{f}[x_m(x'-x'')+y_m(y'-y'')]\}$$

$$\times \exp[-j\frac{k_0(z'-z'')}{2f^2}({x_m}^2+{y_m}^2)]T(x'+x,y'+y;z')$$

$$\times T^*(x''+x,y''+y;z'')\,|M(x_m,y_m)|^2$$

$$\times dx'dy'dx''dy''dz'\,dz''dx_m dy_m. \tag{5.1-3}$$

This heterodyne current contains the scanned and processed information of the 3-D object. Different processing operations can be expected with the specified selections of the pupils, $p_1(x,y)$ and $p_2(x,y)$, as well as the mask, $M(x,y)$, which is located at the back focal plane of lens L2. As calculated by Indebetouw, Klysubun, Kim, and Poon [2000], the coherency of the two-pupil scanning system can be modified by changing the mask, $M(x_m,y_m)$. We shall summarize the results of Eq. (5.1-3) for $M(x_m,y_m)=1$ and $M(x_m,y_m)=\delta(x,y)$.

For the mask being an open mask, i.e., $M(x,y)=1$, Eq. (5.1-3) becomes

$$i_\Omega(t) \propto \mathrm{Re}\Big[\int P_1^*(x',y';z+z_0)P_2(x',y';z+z_0)$$

$$\times |T(x'+x,y'+y;z)|^2\,dx'dy'dz\,\exp(j\Omega t)\Big]. \tag{5.1-4}$$

This equation is basically identical to Eq. (3.4-5), which corresponds to incoherent processing, because only the intensity values, i.e., $|T|^2$, are processed. However, note that the intensity can be processed by the two pupils, $p_1(x,y)$ and $p_2(x,y)$.

On the other hand, for a pinhole mask centered on the axis, i.e., $M(x,y)=\delta(x,y)$. Equation (5.1-3) then becomes

$$i_\Omega(t) \propto \mathrm{Re}\Big[[\int P_2(x',y';z'+z_0)T(x'+x,y'+y;z')\,dx'dy'dz']$$

$$\times [\int P_1^*(x'',y'';z''+z_0)T^*(x''+x,y''+y;z'')\;dx''dy''dz'']\exp(j\Omega t)\Big].$$

For a specific case, if we let $p_1(x,y)=\delta(x,y)$, i.e., one of the scanning beams is a uniform plane wave, and leave $p_2(x,y)$ as is, then $\int_{-\infty}^{\infty}P_1^*(x'',y'';z''+z_0)T^*(x''+x,y''+y;z'')\;dx''dy''dz''$ is a constant, and the above equation becomes

$$i_\Omega(t) \propto \mathrm{Re}\Big[\int [P_2(x',y';z+z_0)$$

$$\times T(x'+x, y'+y; z)\, dx'dy'dz\,] \exp(j\Omega t)\Big]. \qquad (5.1\text{-}5)$$

We see that we can process the object's amplitude transmittance by pupil $p_2(x, y)$. Equations (5.1-4) and (5.1-5) represent the important results of the generalized two-pupil heterodyne scanning image processor. By varying the detection mode from pinhole to spatially integrating detection, we are able to change the coherence property of the imaging process of a 3-D object from linear in intensity [see Eq. (5.1-4)] to linear in amplitude [see Eq. (5.1-5)]. By varying the size of the mask, it is possible to obtain 3-D *partial coherent image processing* [Poon and Indebetouw (2003)].

By incorporating Eq. (5.1-4) and (5.1-5) into one simple important result, we have

$$i_\Omega(t) \propto \text{Re}[\, i_{\Omega p}(x, y) \exp(j\Omega t)], \qquad (5.1\text{-}6a)$$

where, for $M(x, y) = \delta(x, y)$ and $p_1(x, y) = \delta(x, y)$ we have the following coherent processing equation,

$$i_{\Omega p}(x, y) = \int P_2(x', y'; z + z_0) T(x'+x, y'+y; z)\, dx'dy'dz. \qquad (5.1\text{-}6b)$$

For $M(x, y) = 1$, we have the incoherent processing equation,

$$i_{\Omega p}(x, y) = \int P_1^*(x', y'; z + z_0) P_2(x', y'; z + z_0) \times |T(x'+x, y'+y; z)|^2\, dx'dy'dz. \qquad (5.1\text{-}6c)$$

Again T or $|T|^2$ is the input object that is being scanned and it can be a complex amplitude object or intensity object. $i_\Omega(t)$ is the scanned and processed heterodyne output current at a temporal frequency of Ω from the photodetector, and $i_{\Omega p}(x, y)$ is in general a complex function. Hence, the amplitude and the phase of the heterodyne current, $i_\Omega(t)$, carry the complete processed information.

The scanned and processed current can be demodulated according to Fig. 5.1 under the usual multiplexing electronic detection, and this gives the following two outputs:

$$i_c(x, y) \propto |i_{\Omega p}(x, y)| \sin(\theta), \qquad (5.1\text{-}7a)$$

and

$$i_s(x, y) \propto |i_{\Omega p}(x, y)| \cos(\theta), \qquad (5.1\text{-}7b)$$

where $i_{\Omega_p}(x,y) = |i_{\Omega_p}(x,y)|\exp[j\theta(x,y)]$. Processing operations can be manipulated by the selected choice of pupils, $p_1(x,y)$ and/or $p_2(x,y)$, according to Eq. (5.1-6).

These important results open up new avenues for unconventional imaging. For one, coherent processing has been recently assessed experimentally [Indebetouw, Tada and Leacock (2006)], and the other is its ability to perform 3-D coherent image processing. In the case of incoherent processing, we can perform *3-D complex incoherent image processing*. The term "3-D" means the object being processed can be of a 3-D nature, and the term "complex" means that the processing element for the intensity object can be represented by a complex function [see Eq. (5.1-4) as the processing element is $P_1^* P_2$]. Thus, we have mentioned some of the virtually unexplored topics in 3-D optical image processing [Poon and Indebetouw (2003)].

Example 5.1 Holographic Recording in Coherent Mode

For coherent processing, we will use Eq. (5.1-6b). In general, $T(x,y;z)$ is processed by selecting $p_2(x,y)$. For a simple holographic recording, we select $p_2(x,y) = 1$. For this selection, according to Eq. (5.1-1b) and by using Table 1.1 and Eq. (2.3-11), $P_2(x,y;z+z_0)$ becomes

$$\begin{aligned} P_2(x,y;z+z_0) &= \mathcal{F}\{p_2(x,y)\}_{k_x=\frac{k_0 x}{f},k_y=\frac{k_0 y}{f}} * h(x,y;z+z_0) \\ &= 4\pi^2\delta(\tfrac{k_0 x}{f},\tfrac{k_0 y}{f}) \\ &\quad * \Big\{\exp[-jk_0(z+z_0)]\ \frac{jk_0}{2\pi(z+z_0)}\exp\Big[\frac{-jk_0\,(x^2+y^2)}{2(z+z_0)}\Big]\Big\} \\ &\propto \exp[-jk_0(z+z_0)]\ \frac{jk_0}{2\pi(z+z_0)}\exp\Big[\frac{-jk_0\,(x^2+y^2)}{2(z+z_0)}\Big]. \end{aligned} \quad (5.1\text{-}8)$$

By substituting Eq. (5.1-8) into Eq. (5.1-6b), we now have

$$\begin{aligned} i_{\Omega p}(x,y) &= \int \exp[-jk_0(z+z_0)]\ \frac{jk_0}{2\pi(z+z_0)} \\ &\quad \times \exp\Big[\frac{-jk_0\,(x'^2+y'^2)}{2(z+z_0)}\Big] T(x'+x,y'+y;z)dx'dy'dz \\ &= \int \exp[-jk_0(z+z_0)]\ \frac{jk_0}{2\pi(z+z_0)} \end{aligned}$$

$$\times \left[\left\{ \exp\left[\frac{-jk_0 (x^2+y^2)}{2(z+z_0)} \right] \right\}^* \otimes T(x,y;z) \right] dz$$

according to the definition of correlation. By using Eq. (1.2-5), the above integration can be written in terms of convolution to become

$$i_{\Omega_p}(x,y) = \int \exp[-jk_0(z+z_0)] \frac{jk_0}{2\pi(z+z_0)}$$

$$\times \left[\left\{ \exp\left[\frac{-jk_0 (x^2+y^2)}{2(z+z_0)} \right] \right\} * T(x,y;z) \right] dz. \qquad (5.1\text{-}9)$$

Note that this corresponds to the holographic recording of coherent information, $T(x,y;z)$, because it is clearly shown by comparing it to the incoherent case given by Eq. (3.5-5). Indeed, Eq. (5.1-9) tells us that we have a complex Fresnel zone plate hologram of $T(x,y;z)$.

5.2 Single-Beam Scanning vs. Double-Beam Scanning

Recently, the applicability of optical scanning holography (OSH) to 3-D microscopy has been assessed by taking into account polarization effects, high numerical apertures, and generalized illumination wavefronts [Swoger, Martinez-Corral, Huisken, and Stelzer (2002)]. In low-NA systems, polarization remains the same during light propagation. Polarization is necessarily taken into account when high-NA lenses are used. Generalized illumination refers to the use of the two pupils associated with the two scanning beams. Ideally, one of the pupils is a delta function and the other is unity. This gives a plane wave and a spherical wave on the object, respectively. For arbitrary pupil functions, we have a generalized illumination wavefront on the object [Indeed, for example, Eq. (5.1-4) points to the fact that the object, $|T(x,y;z)|^2$, is actually illuminated by $P_1^* P_2$, thereby providing a generalized illumination].

The authors also use the term "reference beam" and "object beam" when referring to the plane wave and the spherical wave in the ideal case. In addition, a single-beam scanning technique has been proposed and compared to double-beam scanning. *Double-beam scanning* in OSH refers to the fact that the combination of a plane wave and a spherical wave is used to raster scan a thick specimen, while *single-beam scanning* means that only one of the waves is used to scan and the other wave remains stationary with respect to the specimen. Figure 5.2 shows the schematics of the scanning configurations for OSH. For single-beam scanning, mirror M1 is used to scan the beam and mirror M2 is fixed. For double-beam scanning, M2 is used to

scan and M1 is fixed. The specimen and the mask are placed in the front focal plane and in the back focal plane of lens L2, respectively. This corresponds to the situation shown in Fig. 5.1. In the following section, we will summarize some observations made by Swoger et al.

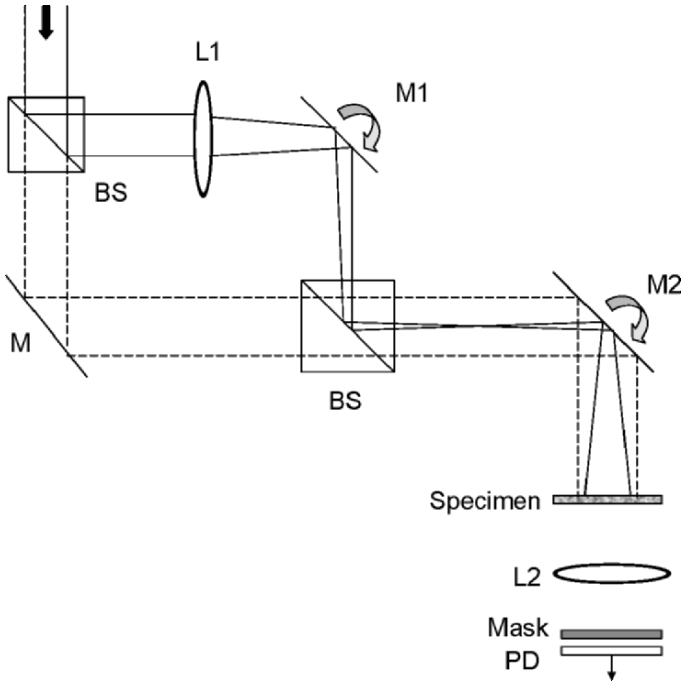

Fig. 5.2 Scanning configurations for optical scanning holography.
(M: mirror, M1,2: scanning mirrors, BS:beamsplitter, L1 and L2: lenses; PD: photodetector).

Regardless of the polarization directions of the two scanning beams, double-beam scanning is well suited for optical scanning holography when working in the incoherent mode (open mask in front of the detector). However, in order to obtain holographic information in a coherent mode (pin-hole mask in front of the detector), it is necessary to have a uniform plane wave as one of the scanning beams on the object. In any case, if the reference beam is a uniform plane wave and the object wave has the same polarization of the plane wave, the results reduce to the conclusion developed earlier by Indebetouw, Klysubun Kim, and Poon [2000]. On the other hand, during single-beam scanning for the coherent mode, there is no need for the reference beam to be uniform and the polarization directions do not need to be constant. The reference beam here now refers specifically to the beam that is not being scanned. However, the incoherent mode is restricted by the constant polarization direction of the reference beam when we attempt to obtain holographic information. Therefore, there are several pros and cons

associated with the two scanning configurations and for future work we should include the actual implementation of a high-NA optical scanning holographic system that is capable of allowing us to observe live biological specimens in both fluorescence and phase contrasts. Recently, optical scanning holographic systems operating in the coherent mode have been implemented to test its phase contrast capabilities [Indebetouw, Tada, and Leacock (2006)]. To end this section, I also want to point out that recent experiments have been demonstrated by using single-beam scanning [Chien, Dilworth, Liu and Leith (2006)]. The authors consider the term "scanning holography" and "synthetic-aperture optics" to be essentially interchangeable because both techniques imply phase-preserving scanning. Indeed, it was pointed out as early as the late 1970's in the article by Poon and Korpel [1979] that scanning holographic recording was analogous to *synthetic-aperture radar*.

5.3 PSF Engineering

As pointed out in section 3.6, the basic principle of optical scanning holography is that we simply create the time-dependent Fresnel zone plate (TDFZP) in order to raster scan the object that allows us to obtain holographic information. This can be implemented by the two-pupil heterodyne image processor that was discussed in section 3.4. In the processor, we let the two pupil functions be $p_1(x,y) = 1$ and $p_2(x,y) = \delta(x,y)$ on the pupil plane, as shown in Fig. 5.3a), so that the scanning beam intensity at a distance of z_0 away from the focal point, c, of the lens is given by Eq. (3.6-1) as follows:

$$
\begin{aligned}
& I_{\text{scan}}(x,y;t) \\
& = |\, a\exp[j(\omega_0+\Omega)t] \,+\, \frac{jk_0}{2\pi z_0}\,\exp[-\frac{jk_0(x^2+y^2)}{2z_0}]\exp(j\omega_0 t)|^2, \\
& = \, A + \, B\sin[\frac{k_0}{2z_0}(x^2+y^2)+\Omega t], \qquad (5.3\text{-}1)
\end{aligned}
$$

where it is understood that the two pupils are of different temporal frequencies accordingly. The scanning beam intensity is the time-dependent Fresnel zone plate, and the situation is shown schematically in Fig. 5.3a).

If the object is a pin hole, a delta function mathematically, then the output after electronic detection (for example, multiplying with cosΩt and lowpass filtering) is given by Eq. (3.6-3) as follows:

$$i_c(x,y) \sim \sin[\frac{k_0}{2z_0}(x^2+y^2)]. \qquad (5.3\text{-}2)$$

The result above is the hologram of a pin-hole object for the single channel. For brevity, the channel due to the multiplying with $\sin\Omega t$ and lowpass filtering is not considered here. Upon plane-wave illumination of the hologram, a real image will focus at z_0 in front of the hologram. If the hologram has a limiting aperture size of radius r, then its NA is r/z_0, which gives λ_0/NA as the resolution of the reconstructed point source. This reconstructed point source is the point spread function (PSF) of the system being considered. Now, by manipulating the functional form of the pupils, we can modify the PSF of the system as we see fit. Nowadays, this is known as *PSF-engineering* [Martinez-Corral (2003)].

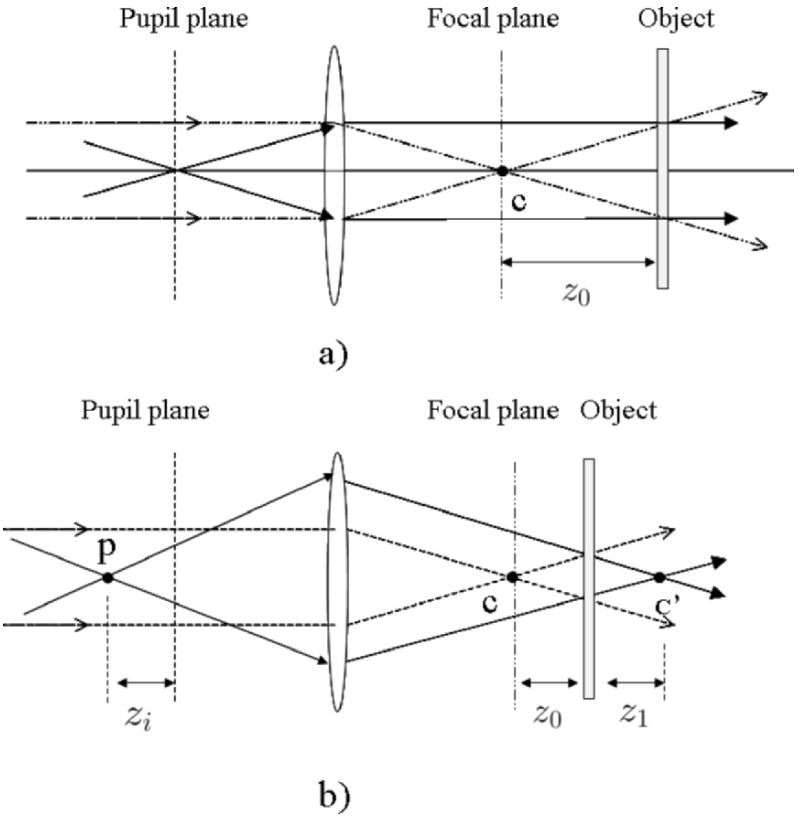

Fig. 5.3a) Optical scanning holography with time-dependent FZP as a scanning beam. b) Optical scanning holography with scanning spherical waves of opposite curvatures. Adapted from T.-C. Poon, J. Holography and Speckle 1, 6 (2004).

Let us consider the following situation. We let $p_1(x,y)=1$ as before, but set $p_2(x,y)=\exp[-\frac{jk_0(x^2+y^2)}{2z_i}]$. We shall find the PSF with these choices of the pupils. We are familiar with the choice of $p_1(x,y)=1$ because it gives a

spherical wave on the object at a distance z_0 away from the focal plane of the lens, which corresponds to the term $\frac{jk_0}{2\pi z_0}\exp[-\frac{jk_0(x^2+y^2)}{2z_0}]\exp(j\omega_0 t)$ in Eq. (5.3-1). The situation is shown in Fig. 5.3b). Let us find what a is in Eq. (5.3-1) for the choice of $p_2(x,y)$ given above. Note that $a(x,y)$ is now a function of x and y. Through the Fourier transformation of the lens [see Eq. (2.4-6)] and Fresnel diffraction at a distance of z_0 [see Eq. (2.3-12)], we can write the field distribution due to $p_2(x,y)$ on the object as

$$a(x,y) = \mathcal{F}_{xy}\{p_2(x,y)\}\Big|_{\substack{k_x=k_0x/f\\k_y=k_0y/f}} * h(x,y;z_0) \tag{5.3-3}$$

$$= \mathcal{F}_{xy}\Big\{\exp[-\frac{jk_0(x^2+y^2)}{2z_i}]\Big\}\Big|_{\substack{k_x=k_0x/f\\k_y=k_0y/f}} * h(x,y;z_0),$$

where f is the focal length of the lens. The above Fourier transformation can be found by using Table 1.1 on page 2. We then perform the convolution and the result, apart from some constant, is given as follows:

$$a(x,y) = \frac{jk_0}{2\pi z_1}\exp[\frac{jk_0(x^2+y^2)}{2z_1}]. \tag{5.3-4}$$

Note that $a(x,y)$ can either be converging wavefronts or divergent wavefronts on the specimen and this is dependent on the location of the focused point, p. In Fig. 5.3b), we show that point c′ is the image point of the focused point, p, and hence the radius of curvature, z_1, is positive in the situation because we have converging wavefronts illuminating the specimen [see Example 2.4 on spherical wave]. The value of z_1 can be designed accordingly by properly locating point p or the distance, z_i, under the imaging condition so that

$$\frac{1}{f+z_i} + \frac{1}{f+z_0+z_1} = \frac{1}{f}. \tag{5.3-5}$$

Therefore, we can design $p_2(x,y)$ with a different radius of curvature.

For the choices of $z_i = 2f$ and $z_0 = z_1 = f/4$, Eq. (5.3-5) will be satisfied. Since $z_0 = z_1$, we will have spherical waves of opposite curvatures illuminating the specimen. Hence, with Eq. (5.3-4) and $z_0 = z_1$, the scanning beam intensity becomes

$$I_{\text{scan}}(x,y;t)$$

$$\propto |\exp[\frac{jk_0(x^2+y^2)}{2z_0}]\exp[j(\omega_0+\Omega)t] + \exp[-\frac{jk_0(x^2+y^2)}{2z_0}]\exp(j\omega_0 t)|^2$$

$$= A' + B' \sin[\frac{k_0}{2(z_0/2)}(x^2 + y^2) + \Omega t], \tag{5.3-6}$$

where A' and B' are some constants. The above scanning beam gives

$$i_c(x, y) \sim \sin[\frac{k_0}{z_0}(x^2 + y^2)] \tag{5.3-7}$$

as our new hologram for the selected pupils. Upon real image reconstruction of the hologram given by Eq. (5.3-7), we see that the image is formed at a distance of $z_0/2$. For the same limiting aperture size of the hologram, r, similar to the standard optical scanning setup, its NA now becomes $r/(z_0/2)$. This gives $\lambda_0/(2NA)$ as the resolution of the reconstructed point source, which is our new PSF. The result means that for the same hologram aperture size, it is possible to synthesize the point-spread function in optical scanning holography in order to obtain holographic reconstructions with a transverse resolution exceeding the Rayleigh limit of the aperture up to a factor of 2, at least in the limit of low NA. Indeed, this has been investigated by Indebetouw (2002) and was recently confirmed by optical experiments [Indebetouw, Maghnouji, and Foster (2005)]. Other pupils examined so far include *axicons*, which have been used to achieve optical sectioning, however, thus far only simulations have been provided [Indebetouw, Zhong, and Chamberlin-Long (2006)].

In general, arbitrary complex amplitude distributions of the pupils can be synthesized by using masks, refractive or diffractive optical elements (DOEs), or spatial light modulators which allow dynamic changes. For $p_2(x, y) = \exp[-\frac{jk_0(x^2+y^2)}{2z_0}]$ shown in this example, we can simply implement it by placing a point source at a distance, z_i, in front of the pupil plane as shown in Fig. 5.3b). In general, I want to point out that the two-pupil method offers a broad range of possibilities when synthesizing unconventional PSFs for potential novel applications. One of the new applications is *super-resolution* [Indebetouw, Tada, Rosen and Brooker (2007)].

References

5.1 Chien, W.-C., D. S. Dilworth, E. Liu, and E. N. Leith (2006). "Synthetic-aperture chirp confocal imaging," *Applied Optics* 45, 501-510.

5.2 Cuche, E., F. Bevilacqua, and C. Depeursinge (1999). "Digital holography for quantitative phase-contrast imaging," *Optics Letters* 24, 291-293.

5.3 Indebetouw, G. (2002). "Properties of a scanning holographic microscope: improved resolution, extended depth of focus, and/or optical sectioning," *Journal of Modern Optics* 49, 1479-1500.

5.4 Indebetouw, G., P. Klysubun, T. Kim, and T.-C. Poon (2000). "Imaging properties of scanning holographic microscopy," *Journal of the Optical Society of America A* 17, 380-390.

5.5 Indebetouw, G., A. El Maghnouji, and R. Foster (2005). "Scanning holographic microscopy with transverse resolution exceeding the Rayleigh limit and extended depth of focus," *Journal of the Optical Society of America A* 22, 829-898.

5.6 Indebetouw, G., Y. Tada and J. Leacock (2006). "Quantitative phase imaging with scanning holographic microscopy: an experimental assessment," available at http://www.biomedical-engineering-online.com/content/5/1/63.

5.7 Indebetouw, G., W. Zhong, and D. Chamberlin-Long (2006). "Point-spread function synthesis in scanning holographic microscopy," *Journal of the Optical Society of America A* 23, 1708-1717.

5.8 Indebetouw, J., Y. Tada, J. Rosen, and G. Brooker (2007). "Scanning holographic microscopy with resolution exceeding the Rayleigh limit of the objective by superposition of off-axis holograms," *Applied Optics*, to appear.

5.9 Martinez-Corral, M. (2003). "Point spread function engineering in confocal scanning microscopy," *Proceedings of SPIE*, Vol. 5182, 112-122.

5.10 Poon, T.-C. and A. Korpel (1979). "Optical transfer function of an acousto-optic heterodyning image processor," *Optics Letters* 4, 317-319.

5.11 Poon, T.-C. (2004). "Recent progress in optical scanning holography," *Journal of Holography and Speckle* 1, 6-25.

5.12 Poon, T.-C. and G. Indebetouw (2003). "Three-dimensional point spread functions of an optical heterodyne scanning image processor," *Applied Optics* 42, 1485-1492.

5.13 Swoger, J., M. Martínez-Corral, J. Huisken, and E. H. K. Stelzer (2002). "Optical scanning holography as a technique for high-resolution three-dimensional biological microscopy," *Journal of the Optical Society of America A* 19, 1910-1918.